

Article

Microgravity as an Anti-Metastatic Agent in an In Vitro Glioma Model

Maurizio Sabbatini * , Valentina Bonetto, Valeria Magnelli , Candida Lorusso , Francesco Dondero  and Maria Angela Masini

Department of Science and Innovation Technology (DISIT), Università del Piemonte Orientale—Via T. Michel 11, 15121 Alessandria, Italy; valentina.bonetto@uniupo.it (V.B.); valeria.magnelli@uniupo.it (V.M.); candida.lorusso@uniupo.it (C.L.); francesco.dondero@uniupo.it (F.D.); maria.masini@uniupo.it (M.A.M.)

* Correspondence: maurizio.sabbatini@uniupo.it

Abstract: Gravity is a primary physical force that has a profound influence on the stability of the cell cytoskeleton. In our research, we investigated the influence of microgravity on altering the cytoskeletal pathways of glioblastoma cells. The highly infiltrative behavior of glioblastoma is supported by cytoskeletal dynamics and surface proteins that allow glioblastoma cells to avoid stable connections with the tissue environment and other cells. Glioblastoma cell line C6 was exposed to a microgravity environment for 24, 48, and 72 h by 3D-RPM, a laboratory instrument recognized to reproduce the effect of microgravity in cell cultures. The immunofluorescence for GFAP, vinculin, and Connexin-43 was investigated as signals related to cytoskeleton dynamics. The polymerization of GFAP and the expression of focal contact structured by vinculin were found to be altered, especially after 48 and 72 h of microgravity. Connexin-43, involved in several intracellular pathways that critically promote cell motility and invasion of glioma cells, was found to be largely reduced following microgravity exposure. In conclusion, microgravity, by reducing the expression of Connexin-43, alters the architecture of specific cytoskeletal elements such as GFAP and increases the focal contact, which can induce a reduction in glioma cell mobility, thereby inhibiting their aggressive metastatic behavior.

Keywords: astrocytes; GFAP; vinculin; Connexin-43; 3D-RPM



Citation: Sabbatini, M.; Bonetto, V.; Magnelli, V.; Lorusso, C.; Dondero, F.; Masini, M.A. Microgravity as an Anti-Metastatic Agent in an In Vitro Glioma Model. *Biophysica* **2023**, *3*, 636–650. <https://doi.org/10.3390/biophysica3040043>

Academic Editor: Danilo Milardi

Received: 19 October 2023

Revised: 21 November 2023

Accepted: 23 November 2023

Published: 25 November 2023



Copyright: © 2023 by the authors. Licensee MDPI, Basel, Switzerland. This article is an open access article distributed under the terms and conditions of the Creative Commons Attribution (CC BY) license (<https://creativecommons.org/licenses/by/4.0/>).

1. Introduction

Gravity is a fundamental physical force that has a strong impact on all life forms existing on Earth and their biological processes. With the advent of space programs, interest in the effects of microgravity on human cells has grown since the initial investigations performed within the US Skylab program in the early 1970s. The spaceflight results show that cells are very sensitive to gravitational changes, revealing alterations in cell morphology [1], proliferation and differentiation [2], apoptosis [3], cell adhesion, and the corresponding signaling pathways [4]. The availability of a new tool to mimic the microgravity environment has renewed interest in the effects of microgravity on cell biology, increasing the possibility of performing experiments without space missions. The 3D-Random Positioning Machine (3D-RPM) is a device consisting of two gimbal-mounted frames that constantly rotate biological samples around two perpendicular axes. This device simulates some of the physical effects of space flight by providing a vector-averaged reduction (10^{-6} g) in the apparent gravity, generating low levels of shear forces [5,6]. Experiments on the RPM have shown results comparable to space-flown experiments in several studies [4,5,7].

The first studies that dealt with the effects of microgravity on human cancer cells revealed alterations in cell proliferation, survival, and apoptosis, driving the cells towards a less aggressive phenotype. These alterations are probably linked to cytoskeleton modifications, which function as gravity sensors for the cells [8,9].

However, further studies have also pointed out the role of microgravity in favor of carcinogenesis processes. Researchers have found some evidence showing that microgravity may accelerate cancer progression in leukemia, as well as lung, breast, ovarian, liver, head, and neck cancers [10–12].

These findings indicate microgravity's role as a two-edged sword in cancer [13], limiting the initial enthusiasm for it.

However, though several studies reported the effects of microgravity on the proliferative pathways of cancer cells, less is known concerning their metastatic behavior. It has been seen that microgravity promotes cellular migration for non-small cell lung cancer cells [14]. On the contrary, simulated microgravity reduces the metastatic strength of human lung adenocarcinoma, inhibiting migration and invasion [15]. Exposure to long-term microgravity has been related to a reduced aggressiveness of thyroid cancer cells [16].

Metastasis is a very complex process that is based on a prominent reorganization of the cytoskeleton, involving extensive crosstalk between different components [17]. The optimal dynamism of the cytoskeleton is the basis for cellular migration, and it is a critical point in cancer cell metastases. The cytoskeleton is thought to be a major factor for cellular graviperception, and microgravity affects the dynamic organization of the cells, inducing impairment in several cytoskeleton-dependent pathways [4,9,18,19].

Focal adhesions have been found to play an important role in the inhibition of proliferation and metastasis in melanoma cells [20].

For these areas, gravity alteration has attracted renewed interest as potential tools for limiting the metastatic behavior of cancer cells, especially in those cell types in which cytoskeleton dynamics represent the main factor in metastatic and proliferative behaviors [4,17]. Among several cell types that are strongly dependent on their physiological performance in cytoskeletal roles, we chose glioblastoma cells, which derive from the cancerogenic transformation of astrocytes.

Glioblastoma is the most frequent type of primary brain tumor. It strongly reduces life expectancy, with most patients dying within 16–20 months after the diagnosis, despite all of the advanced therapy available [21,22]. Glioblastoma is a rapidly growing and highly infiltrative malignant tumor, which propagates primarily along the white matter fiber tracts and infiltrating grey matter during the advanced stage [23].

The highly infiltrating behavior of glioblastoma inside the brain parenchyma is widely supported by high cytoskeleton dynamicity and surface proteins that allow the glioblastoma cells to avoid stable connections with the tissue environment and neighboring cells, such as neurons and other astrocytes [4]. The viability and migration properties of a glioma cell line were inhibited using simulated microgravity upon the depression of FAK intracellular signaling [24].

The aim of the present research is to analyze the effects of microgravity on the survival and integrity of cytoskeletal patterns and cell–cell connecting factors following long-term microgravity exposure in C6 glioma cells, in order to highlight the potential reducing effect of microgravity on glioma aggressive behavior.

In the present study, the C6 glioma cell line was chosen because it is considered to be a gold standard in glioma research. C6 cells are developed experimentally by inducing tumoral alterations in the astrocytes of Wistar rats. C6 cells exhibit the same histological features as human glioblastoma cells, and have shown a high grade of tissue invasion [25].

2. Results

The F, G, and M cell groups did not statistically differ from each other for the parameters analyzed. These findings do not allow us to separate gravitational from fluid dynamic effects.

From now on, throughout the study, we refer to the control groups considered invariably as the frame, ground, and moving-ground controls.

Under our experimental conditions, no multicellular component formation was observed, and an evaluable floating cell number was present only after 72 h of microgravity

exposure. The proliferation analysis and cell death yielded similar results to those observed in the adherent cells. The low number of floating cells did not allow Western blot analysis to be performed. The immunohistochemistry analysis displayed similar pictures to those observed in the adherent cells. Therefore, floating cells were no longer considered in the present research.

2.1. Proliferation and Cell Death

Microgravity induced a slowdown in cell proliferation; in particular, cell proliferation was largely affected after 48 and 72 h of microgravity exposure (Figure 1a).

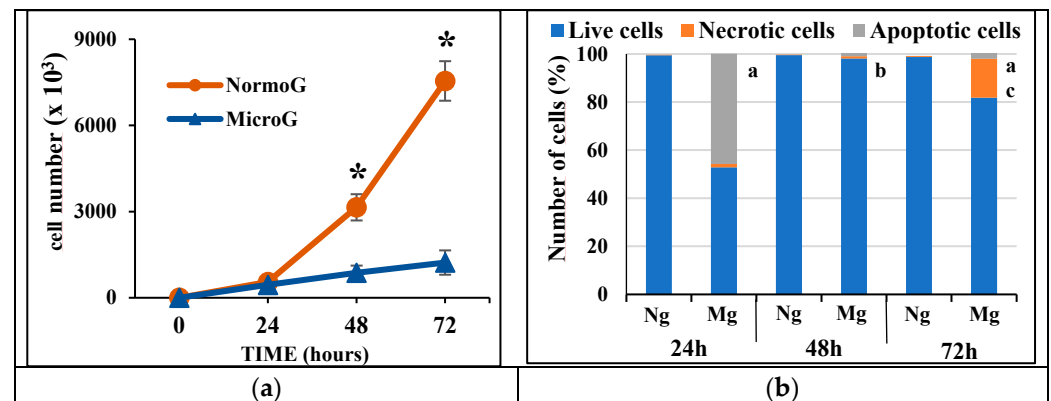


Figure 1. (a) Linear graph showing the proliferation of cells following microgravity exposure. NormoG = normogravity; MicroG = microgravity; * = $p < 0.05$ vs. MicroG. (b) Cytofluorimetric analysis of apoptotic and necrotic cell death following microgravity exposure. a = $p < 0.05$ vs. Ng of isotemporal group; b = $p < 0.05$ vs. 24 h; c = $p < 0.05$ 24 h and 48 h; Ng = normogravity; Mg = microgravity.

Microgravity affected the cell viability after 24 h, inducing cell apoptosis. The observed cellular apoptosis was mainly characterized by an early form of apoptosis as revealed by the cell annexin-V positive/propidium iodide negative (almost 60% of apoptotic cells). Then, after 72 h, the C6 cell population became affected by only necrotic cell death. These findings indicate that C6 cells at 24 h are in a preliminary susceptible phase that may be linked to their proliferative tendency, becoming largely affected by microgravity. Instead, over time, the surviving cells became more resistant (Figure 1b) and characterized by very low proliferation (Figure 1a).

2.2. GFAP

GFAP is the main specific component of the astrocytes' cytoskeletons. However, it does not represent a mere structural element of the cells; it is also involved in cellular adhesion, cell–cell or cell–extracellular matrix (ECM) interrelationships and signaling pathways, revealing the GFAP dynamics as fundamental for the biology of astrocytes in physiological or pathological conditions [26].

In the C6 cells exposed to normogravity after 24 h, the GFAP appears as a homogeneously dispersed matrix into the cytoplasm, without showing correct polymerization into cytoskeletal bundles. GFAP filaments appeared polymerized in well-visible bundles only after 48 h, with an evident organization at 72 h of exposure (Figure 2A–C). This late polymerization of the specific intermediate filaments of C6 cells is compatible with their tumoral nature, inducing a late stabilization of cell morphology.

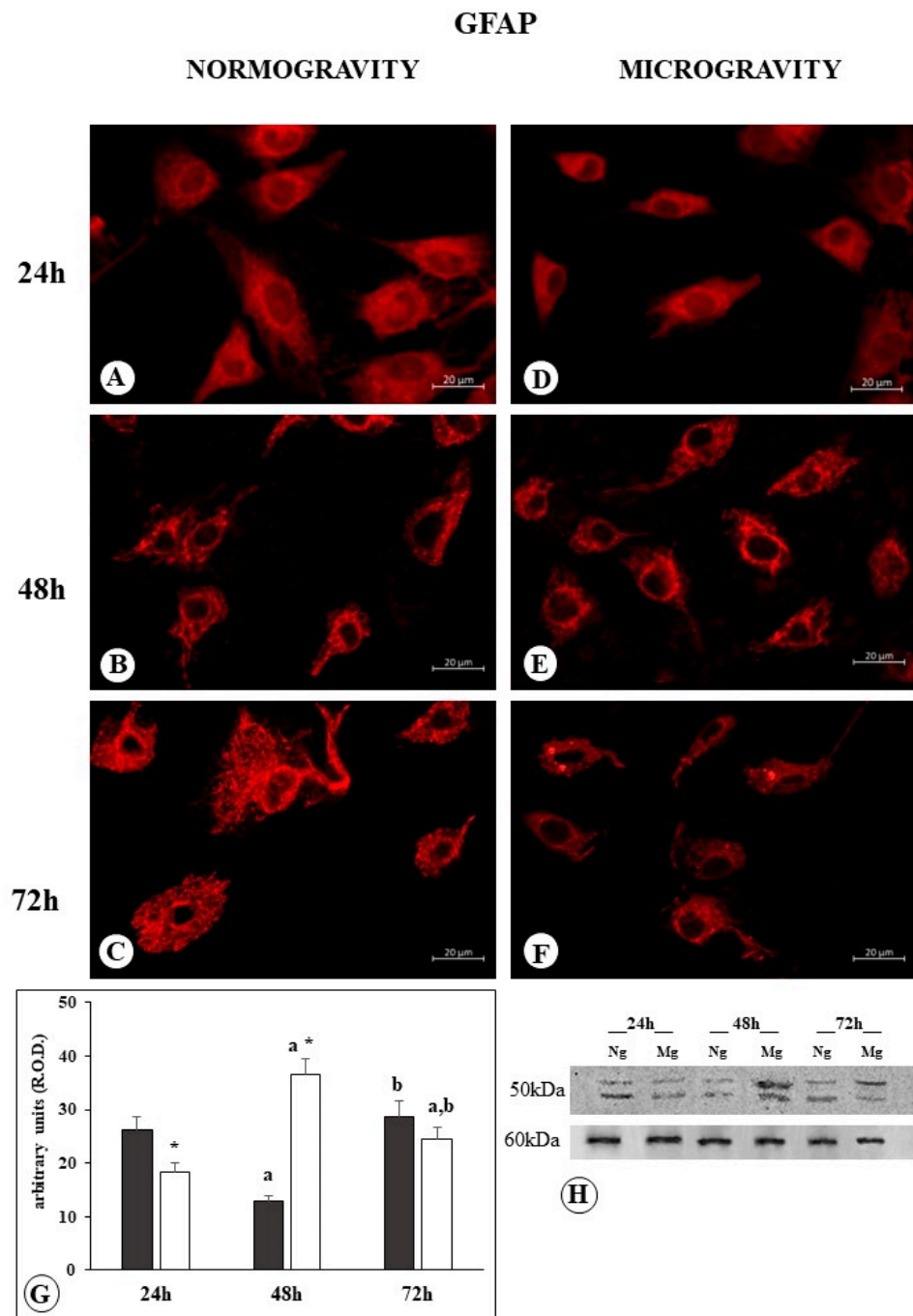


Figure 2. Microphotograph panel illustrating the immunofluorescence localization of GFAP in C6 glioma cells following normogravity ((A–C); Ng) or microgravity ((D–F); Mg). The quantitative expression of GFAP is shown in the bar graph (G) and Western blot panel (H). Black bar = GFAP expression in normogravity; white bar = GFAP expression in microgravity; relative optical density (R.O.D.) see the Section 4. $a = p < 0.05$ vs. 24 h; $b = p < 0.05$ vs. 24 h; $* = p < 0.05$ vs. isotemporal normogravity.

Western blot analysis showed the polymerization of GFAP in a well-defined bundle, seen after 48 h under normogravity conditions, is accompanied by a reduction in the total amount of protein, which increases with increasing bundle polymerization, as can be seen after 72 h (Figure 2G,H).

Following 24 h of microgravity exposure, GFAP appeared in a homogeneously dispersed matrix, gathered in a dense ring around the nucleus, and only faintly dispersed into

the cytoplasm. Following 48 h of microgravity exposure, GFAP filaments appeared as short bundles irregularly branching around the cell cytoplasm. Lastly, at 72 h, the GFAP became organized into a condensed mass with shorter bundles (Figure 2D–F).

Western blot analysis showed that the GFAP amount reduced after 24 h of microgravity exposure, in comparison to the normogravity-exposed cells, indicating that the different disposition of finely dispersed filaments around the nucleus is accompanied by a reduction in GFAP content. Instead, following 48 h of microgravity exposure, the increase in GFAP became clearly evident, whereas following 72 h, only a modest increase in GFAP was detected (Figure 2G,H). These increases in GFAP accompany the observed irregular organization of GFAP into short bundles and condensed masses (Figure 2E,F).

2.3. Vinculin

Vinculin is an important factor in stabilizing the protein complex of focal adhesion, optimizing cell–cell or cell–substrate adhesion. It is present in the cell in two forms [27], a linear form that typically presents in focal adhesion complexes, displayed under microscopic analysis as dot spots along cell borders, and a folded free form inside the cytoplasm, resulting in a diffuse cytoplasm-positive reaction.

The C6 cells exposed to normogravity showed several adhesion contacts at the ends of cell elongation profiles and distributed along the cellular profile. Immuno-positive reaction was faintly detectable inside the cytoplasm, probably related to the vinculin folded form (Figure 3A). No significant differences were observed between cells after 24 h, 48 h, and 72 h of normogravity exposure.

Western blot analysis confirmed the occurrence of the same amount of protein in C6 cells exposed to normal gravity after 24 h, 48 h, and 72 h (Figure 3E,F).

Following C6 exposure to microgravity, no change was observed after 24 h (Table 1); we observed after 48 h an increase in the number of vinculin-positive focal contacts, and a lower diffuse positive reaction inside the cytoplasm (Figure 3B, Table 1). Following 48 h, the vinculin immune-positive distribution inside the cytoplasm increased, and focal contact immunopositive spots appeared larger and reduced in number in comparison to what was observed after 24 h of microgravity (Figure 3B,C and Table 1); furthermore, they were no longer detectable after 72 h of microgravity (Figure 3D). Following 72 h of microgravity exposure, the vinculin immune-positive distribution inside the cytoplasm further increased, displaying an appearance similar to what was observed in normogravity (Figure 3A,D), whereas the focal contacts increased in number (Table 1).

Table 1. Number of vinculin dot spots.

Number/Single Cells	24 h	48 h	72 h
Normogravity	23 ± 8	24 ± 10	22 ± 9
Microgravity	25 ± 10	16 ± 7 *§	48 ± 10 **§

* = $p < 0.05$ vs. 24 h; ** = $p < 0.05$ vs. 24 and 48 h; § = $p < 0.05$ vs. normogravity.

Western blot analysis after 24 and 48 h of microgravity exposure showed a total vinculin content that was similar to the control group. In contrast, a higher vinculin content was observed following 72 h of microgravity in comparison to the other experimental groups (Figure 3E,F).

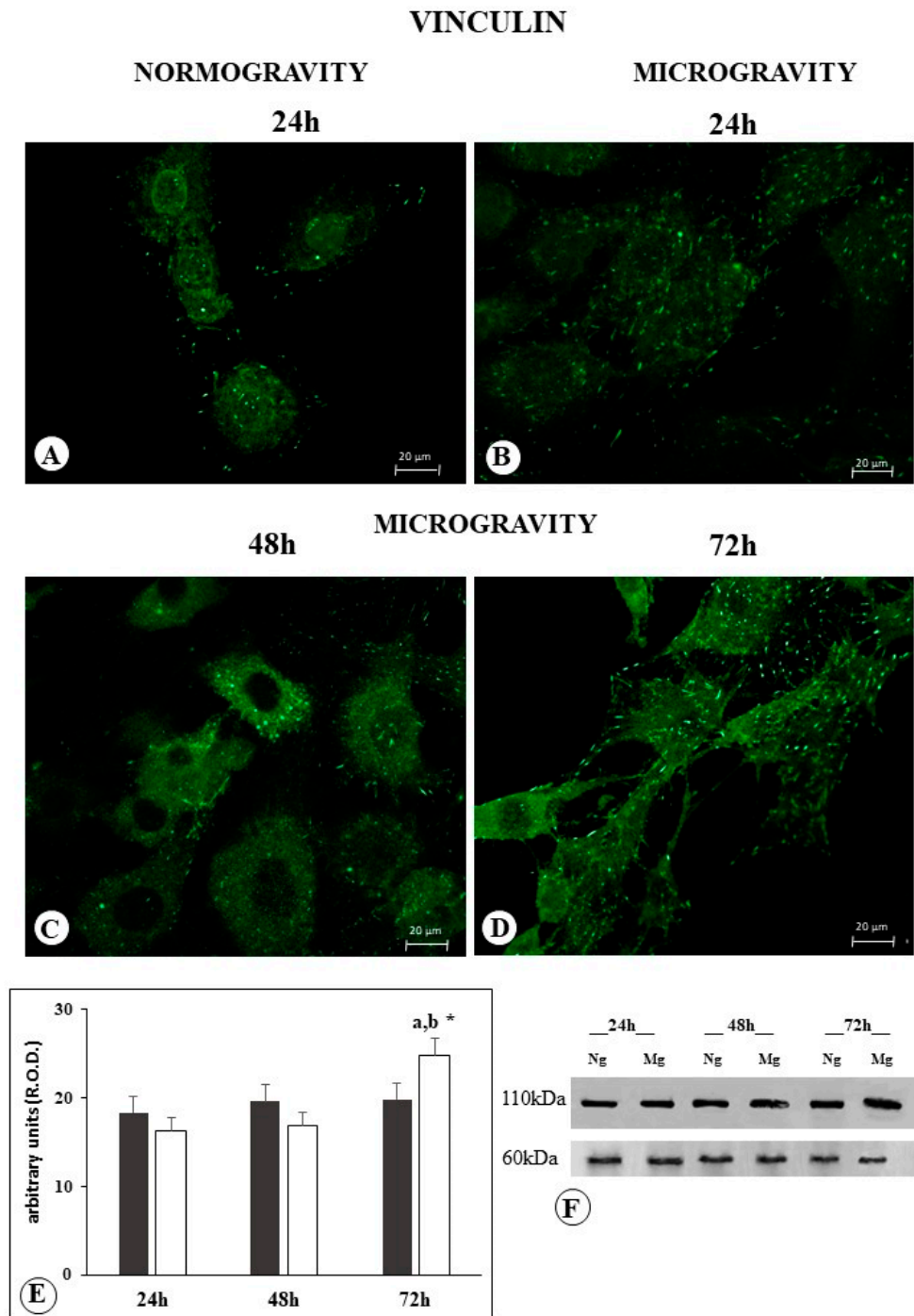


Figure 3. Microphotograph panel illustrating the immunofluorescence localization of vinculin in C6 glioma cells following normogravity ((A); Ng) or microgravity ((B–D); Mg). The quantitative expression of vinculin is shown in the bar graph (E) and the Western blot panel (F). Black bar = vinculin expression in normogravity; white bar = vinculin expression in microgravity; relative optical density (R.O.D.) see Section 4. a = $p < 0.05$ vs. 24 h; b = $p < 0.05$ vs. 24 h; * = $p < 0.05$ vs. isotemporal normogravity.

2.4. Connexin

Connexin (Cx43) is a widely diffuse protein in astrocyte cells and C6 glioma cells, where it is involved in gap junction structure. Furthermore, it forms hemichannels that relate the cell and its extracellular medium. Cx43 was also observed in cytoplasmatic localization in tumor cell lines [28].

The C6 cells exposed to normal gravity for 24 h showed an evident expression of Cx43 visualized as well-defined membrane placoids, and a diffuse cytoplasm positive reaction (Figure 4A). Following 48 h of normogravity, the membrane placoids did not become more visible, whereas a cytoplasm positive reaction of granular appearance can be observed (Figure 4B). After 72 h, a further reduction in the cytoplasm positive reaction was observed (Figure 4C).

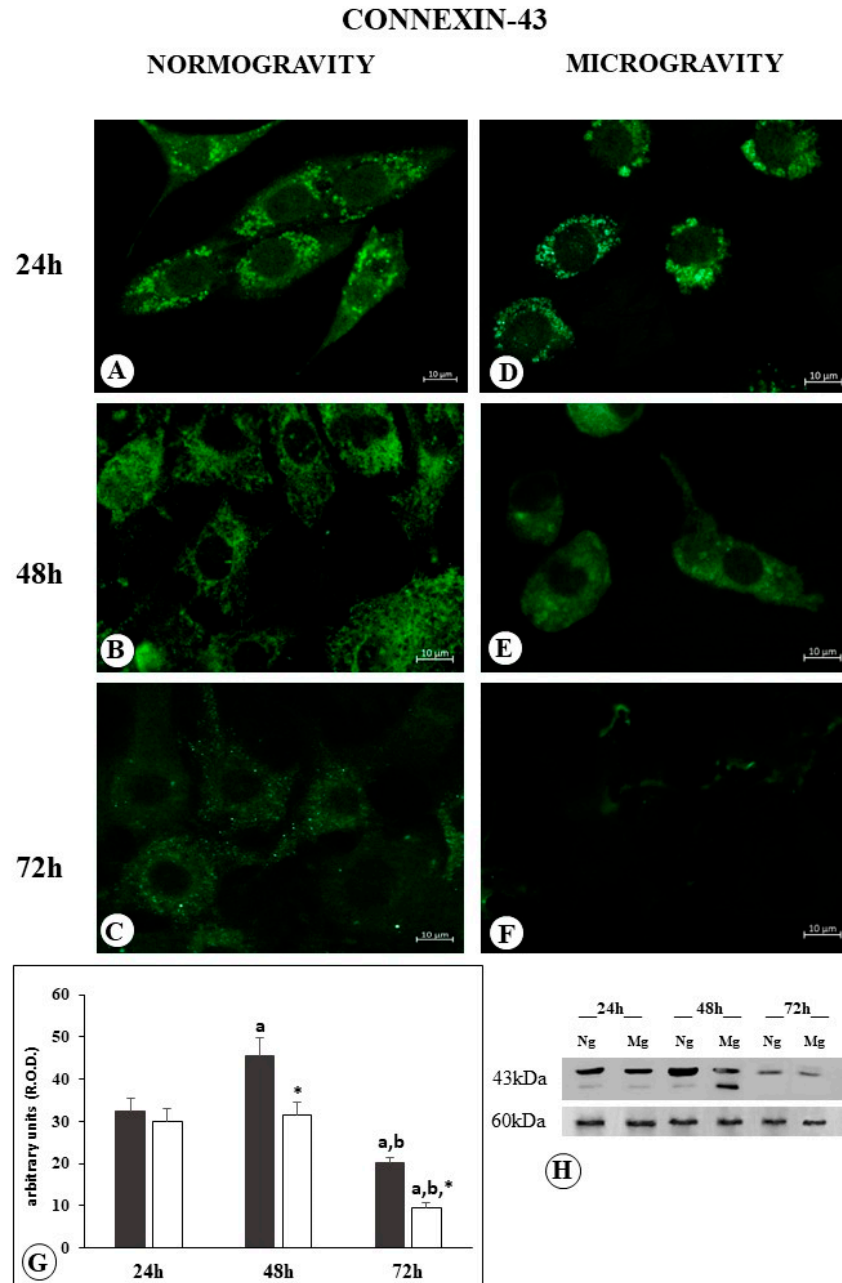


Figure 4. Microphotograph panel illustrating the immunofluorescence localization of Connexin-43 in C6 glioma cells following normogravity ((A–C); Ng) or microgravity ((D–F); Mg). The quantitative expression of Connexin-43 is shown in the bar graph (G) and Western blot panel (H). Black bar = Connexin-43 expression in normogravity; white bar = Connexin-43 expression in microgravity; relative optical density (R.O.D.) see Section 4. $a = p < 0.05$ vs. 24 h; $b = p < 0.05$ vs. 24 h; $* = p < 0.05$ vs. isothermal normogravity.

Following 24 h of microgravity application, Cx43 membrane placoids increased in size, apparently reduced in number, and no appreciable change in the cytoplasm positive reaction was observed (Figure 4D).

Following 48 h of microgravity application, the membrane placoids were not visible anymore, even if a fairly appreciable diffuse cytoplasm positive reaction was still detected (Figure 4E).

The samples observed after 72 h of microgravity revealed the absence of membrane placoids, together with a strong reduction in the cytoplasm positive reaction (Figure 4F).

Western blot analysis revealed a similar amount of protein in Cx43 membrane placoids compared to cells subjected to 24 h in normogravity and in microgravity. Following 48 h in normogravity, the cells are characterized by an increase in Cx43 protein amount, while the microgravity group remains with the similar amount observed after 24 h. The different fragmentation pattern observed in this experimental group may indicate the occurrence of a different structural expression of Cx43 (Figure 4H).

After 72 h, the amount of protein resulted largely decreased, much more in the cells exposed to microgravity than cells exposed to normogravity (Figure 4G,H).

3. Discussion

The cytoskeleton has a key role in the life of cells. It is not only the major determinant of the structural shape of the cell, but it allows for cell movement, and partially mediates crosstalk with the extracellular matrix. In tumor formation, one of the main characteristics of transformed cells is a metastatic behavior consisting of the ability to reduce connections with the extracellular matrix, giving rise to invasive progression towards different organ districts. This last point is heavily affected by cytoskeletal alteration [17].

GFAP represents the main protein of intermediate filaments characterizing astrocytes' cytoskeletons, whose expression and modulation are strictly related to physiological and pathological conditions of astrocytes, including tumoral transformation [26].

Glioma metastatic behavior is mainly characterized by an invasion of the surrounding tissue. Cultured C6 cells exhibit a first phase in which GFAP, the most specific cytoskeleton component, transforms from a dispersed distribution to a well-defined bundle polymerization. We might argue that this reorganization reflects the first phase for C6 tumor cells to assume independence from surrounding environments. Later on (72 h), a well-structured GFAP cytoskeleton may help to drive cell movements towards a metastatic invasion of the surrounding tissue [29]. In the same time-lapse, microgravity exposition causes alterations in the distribution and a different polymerization of GFAP filaments, probably making it difficult for cells to begin their metastatic process.

Vinculin is a key factor in the focal adhesion complex that regulates cell–cell and cell–ECM interactions [30,31]. These interactions are prominent in modulating cell morphology, adhesion, and motility, such as migration and proliferation [32–34]. Consequently, vinculin downregulation promotes cell apoptosis and motility downregulation [35]. Conversely, reduced vinculin expression has been observed to be a distinctive trait in several metastatic cancer cells [36,37]. On the contrary, vinculin has gained a double face value in promoting the metastatic behavior of cancer cells. Cancer cells with high vinculin expression have been found to enter dense tissue matrices, suggesting that matrix stiffness may be responsible in the generation of physical forces promoting tissue invasion [38,39], such as those confirmed in human breast cancer [38] and prostate cancer [40]. On the contrary, in soft tissues such as ovary tissue, the metastatic process is induced by a reduction in vinculin expression [35]. Brain tissue can be considered a soft tissue, and C6 glioma cells have in their vinculin expression reduction one of the promoting factors to metastatic behavior [41]. Experimental evidence indicates that microgravity promotes an increase in vinculin expression in C6 glioma cells, with large amounts of the protein as focal contacts following 24 h of microgravity exposition. After 72 h, a large increase in the number of focal contacts was observed. These findings are compatible with the hypothesis of microgravity as a possible agent able to inhibit the metastatic behavior of glioma cells.

Different scientific papers report that microgravity environments can attenuate the metastatic behaviors of different cancer cells [42] by regulating calcium entry through the Orai1 membrane channels and the SOCE (store-operated-calcium-entry) mechanism. In particular, this has been proven true even for the glioblastoma cell line U87 [43], where the authors claim modeled microgravity as a potential therapeutic strategy in glioblastoma treatment. C6 cells reduce their motility and increase focal adhesion following the silencing of Orai1 channels and decrease in calcium influx [44], which is a possible mechanism for reducing metastatic progression and tumor diffusion.

The altered expression of Connexin-43 (Cx43) has been considered important in sustaining the metabolism of tumor cells; it is considered a key factor in glioblastoma, where its expression is widely linked to metastatic behavior of the tumor [45].

Cx43 is a pleiotropic protein that is not only involved in the architecture of gap junctions, but it also participates in several functions, such as regulation of cell architecture, polarity, mobility, invasion, and growth [45–48]. Cx43 is widely expressed in astrocytes. A decrease in Cx43 expression in glioma cells has been observed, and the levels are inversely correlated with the degree of malignancy [49–51]. However, other studies reported an increase in the invasive action of Cx43-overexpressing glioma cells [48,52]. The enigmatic consequence of Cx43 expression in glioma cells was adequately described by Sin and colleagues, who highlighted the opposing role of Cx43 in glioma progression [53]. Recently, this enigmatic behavior of Cx43 has found an explanation in the research of Hong and colleagues, who evidenced a differential effect of Cx43 in its relationship with surrounding cells so that glioma–glioma Cx43 communication suppresses glioma invasion, while glioma–astrocyte communication favors glioma invasion [54].

In particular, analyses performed on malignant glioma masses reveal that Cx43 is barely expressed, while a much higher level of Cx43 is detected on the plasma membrane of reactive astrocytes surrounding the peritumoral area, and even in tumor cell infiltration and reactive astrocytes [55,56]. These data suggest that the overexpression of Cx43 encourages glioma cell migration and invasion in a gap-junction channel-dependent manner. Similar considerations have been made in the hepatic district, where Cx43 propagates endoplasmic reticulum stress through gap junctions to neighboring hepatocytes [57].

Our findings show differential expression of Cx43 in C6 glioma cells on a time scale ranging between 24 and 72 h. Under normogravity conditions, Cx43 increased the cytoplasmic localization between time zero and 24 h, while we observed a decrease in Cx43 at 48 h, and a further decrease in cytoplasmic localization and recovery of membrane localization at 72 h.

In our experimental set, the isolated condition in which the cells were observed did not allow for a differential comparison of the Cx43 distribution between the core and the periphery of tumoral masses. On the other hand, the pleiotropic and complex effects of Cx43 were well noted.

However, these movements in the expression of Cx43 in C6 cells in normogravity may be considered compatible with the opposing role that Cx43 assumes in glioma biology and metastatic behavior, where loss of expression in the tumor core and increased expression or redistribution of Cx43 at the tumor mass periphery promote infiltration [58].

To this regard, the inhibitory action exerted by microgravity on both cytoplasmic and membrane Cx43 expression highlights the downregulation of one of the main factors linking the metabolism of glioma cells to the surrounding environment.

Cx43 has been reported [59] to control cellular movements through the transcriptional regulation of N-cadherin, by interacting with basic transcription factor 3 (BTF3). BTF3 overexpression has been linked to tumor prognosis, proliferation, and cancer progression. In such a view, reducing Cx43 could impair BTF3 activity, thus reducing interactions with the surrounding tumor microenvironment, opposing the metastatic process.

Mounting evidence has shown a crosstalk between connexins, cytoskeletal, and focal adhesion complexes. In particular, it has been observed that focal adhesion complexes containing vinculin are maintained by the presence of Cx43 that interacts directly with

vinculin [60]. In C6 cells, the increase in Cx43 in the cytoplasm under normogravity may indicate an induced weakness of focal contact, even if the vinculin localization is not altered. This event can be associated with a dynamic modulation of ECM-focal contact interrelationships favoring the metastatic movements of tumoral cells [41].

In turn, Cx43 is also associated with several activation pathways involving cell proliferation, differentiation, survival, and participation widely in mechanical stimuli and cytoskeletal dynamics. We speculate that Cx43 cytoplasmic movement induces the change in GFAP, from a primary cytoskeletal protein that supports astrocyte physiology to a dynamic element that helps tumoral astrocytes move toward tissue invasion.

In this scenario, microgravity exerts its inhibition on Cx43, and its redistribution probably inhibits the primary force, inducing the subsequent dynamic alteration of the other factors investigated.

Ideally, by transporting this vision to *in vivo* conditions, we can speculate that microgravity exerts an inhibitory force on these cell transformation mechanisms, reducing the metastatic progression of C6-type tumoral astrocytes; potentially, this may pave the way for pharmacological interventions that have more time to be effective if the glioma strongly reduces its aggressive behavior.

Limitations of the Study

The present study has several limitations due to the use of *in vitro* cell models that cannot be considered similar to tissue cancer or *in vivo* models, where other factors and interactions with several neighboring cells create a more complex active environment. The 3D-RPM device mimics microgravity; although it is widely considered a cost-effective device [61], it has some limitations in considerations of the effects of shear stress, which needs to be monitored separately, as we have done.

The use of a single tumoral cell line without a comparison with normal cells or other tumor cells limits the possibility of extending our observations more generally, and the behaviors observed in the C6 cells may be closely related only to this cell type. Furthermore, the sample size prevented the analysis of the population effect on the observed mechanisms. In fact, *in vivo*, the presence of a small tumoral size or the presence of a large mass of tumoral cells often activates different behaviors, thus differentiating the response of the core of the tumor mass from the response of the peripheral cells of the tumor mass.

However, a goal of our study is to focus attention on some specific factors that constitute the focal contact, and on the main structural astrocyte protein responsible for the tissue environment-related response (such as GFAP), in determining the influence of microgravity on specific alterations that support the aggressive behavior of glioma cells. Furthermore, a goal of our study is to show that the physical force of gravity is a potential tool to counteract tumor cells that modulate their aggressive behavior by involving pathways of adhesion and movement in the surrounding environment.

4. Materials and Methods

4.1. Culture Procedure

C6 glioma cells, a cell line derived from rat brain tumors, were purchased from ATCC CCL 107, American Tissue Culture Collection, Rockville, MD, USA.

The cells were grown in DMEM medium (Sigma, St. Louis, MO, USA) with the addition of 10% fetal bovine serum and 1% penicillin/streptomycin. The cells were kept at 37 °C in a humidified room with 5% CO₂. For proliferation, cytofluorimetric and Western blot procedure C6 cells were seeded at 500.000 cells/mL in T25 (25 cm²) flasks. For the immunohistochemical procedure, C6 cells were seeded at 50.000 cells/mL using the “slide flask” method (flasks apposed onto tight-fitting removable slides 9.0 cm² in area).

4.2. Simulated Microgravity

The cells were plated in monolayer in flasks, which were subsequently fitted onto a 3D-Random Positioning Machine (3D-RPM, Dutch Space, NL, Leiden, The Netherlands).

The cells were kept at 37 °C in continuous rotation at 56°/s to induce microgravity for 24 h, 48 h, and 72 h. The flasks ($n = 8$) were completely filled with culture medium and placed next to the center of the rotor to minimize centrifugal accelerations.

The frame control flasks (F, 1g, $n = 4$) were placed on the set-up bearing the RPM, in order to monitor the possible vibrations produced by the rotating machinery and transmitted to the holding structure. These frame control flasks were exposed for the same time intervals as above. A second control group named ground flasks (G, 1g, $n = 4$) was kept at 37 °C in a humidified 5% CO₂ incubator, and then analyzed at the same time points as well.

Since the RPM generates limited but present shear forces, especially under adherent cell conditions [62], to differentiate the effect of fluid movements in the flasks, they were settled on a rocking plate. This further control group was named the moving-ground flasks (M, 1g, $n = 4$).

At the end of each experiment, the medium was collected to analyze floating cells separately. The medium was transferred to a 50 mL falcon flask and centrifuged at 1100 rpm for 5 min. the supernatant was discharged, and then forwarded for cell analyses as described below.

The flasks were washed with phosphate buffer saline (PBS, pH 7.4), and the adherent cells were used in the techniques described below.

4.3. Proliferation Assay

The proliferation of C6 cells was evaluated by means of the DNA content. The cells were plated in monolayer in flasks as described above, and after 24 h, the cultures were subjected to simulated μ g (μ g cultures) for 24 h, 48 h, and 72 h. The frame, ground, and moving-ground control groups were set as described above.

Briefly, the medium was removed, and the samples were washed with warm PBS added with 1 mL of lysis solution (urea 10 M, 0.01% SDS in saline sodium citrate buffer [SSC] 0.154 M NaCl, and 0.015 M Na₃C₆H₅O₇ (sodium citrate), pH 7). The cell suspensions were incubated at 37 °C in a shaking bath for 2 h. After that, 1 mL of Hoechst 33258 dye, 1 mg/mL in SSC buffer, was added in the dark. The absorbance was measured with an LS5 Perkin Elmer spectrofluorometer (mod. LS5, Perkin Elmer, Shelton, CT, USA). Cell proliferation was estimated by referring fluorescence units to a linear standard curve for DNA fluorescence versus cell number.

4.4. Analysis of Cell Death

Cell death was determined using FACSCalibur equipment (Becton Dickinson, Franklin Lakes, NJ, USA), then analyzed with FlowJo, LLC (V10, Becton Dickinson, Franklin Lakes, NJ, USA), via the annexin-V/PI assay. The C6 cells were washed with PBS and stained with 5 μ L of annexin V-FITC in 195 μ L of binding buffer for 10 min at room temperature in the dark, then washed with PBS, resuspended in 190 μ L of binding buffer, and stained with 10 μ L of PI. The apoptotic cells were detected as annexin-V-positive cells, while necrotic cells were detected as annexin-V-negative/PI positive cells.

The experiments were performed in triplicate and reported as cell death index, calculated on cell number detected as $100 \times [(\text{microgravity exposure} - \text{control})/\text{control}]$.

4.5. Immunofluorescence and Microscopy Analysis

The cells were fixed in 4% buffered formalin for 15 min at room temperature, and then the slides containing the cultured cells were removed from flasks and evaluated with indirect immunofluorescence. The slides were permeabilized with 0,1% Triton X-100 (Sigma, St. Louis, MO, USA) in PBS, washed in PBS, and then the slides were exposed to normal goat serum (diluted 1:50 in PBS; Sigma Aldrich, St. Louis, MO, USA). For the first step, the fixed cells were incubated at 4 °C overnight with anti-GFAP (mouse monoclonal antibody GA5; dilution 1:100; eBioscience™, San Diego, CA, USA), anti-vinculin (monoclonal antibody 7F9; dilution 1:100; eBioscience™), and anti-Connexin-43 (mouse monoclonal antibody CX-1B1; dilution 1:100; eBioscience™), with primary

antibodies diluted in 1% BSA. The next day, the cells were incubated with eFluor™ 615 and goat anti-mouse (dilution 1:20; eBioscience™) to detect GFAP, and Alexa Fluor 488 goat anti-mouse (dilution 1:25; eBioscience™) to detect vinculin and Connexin-43, for 1.5 h at room temperature. The immunostaining specificity was verified by omitting one of the steps of the immuno-histochemical procedure, or by replacing the primary antisera with non-immune rabbit serum or PBS.

The fluorescence detection was performed with a TCS SP2 confocal microscope (Leica Microsystems, Wetzlar, Germany). The distribution of the targeted proteins was observed, and several images were taken for successive analysis. The vinculin plaques per cell were also determined using Image J software (V.1.52.r).

4.6. Western Blot and Densitometric Analysis

Denaturing electrophoresis was performed on 10–15% gradient polyacrylamide gels (SDS-PAGE). For each sample, 20 µg of total protein was loaded. The protein run was carried out at 30 V for 40 min.

After blotting, nitrocellulose membranes were stained with Red Ponceau, washed with phosphate buffer saline (PBS), and labeled with the primary antibodies against anti-GFAP (mouse monoclonal antibody GA5; dilution 1:200; eBioscience™), anti-vinculin (mouse monoclonal antibody 7F9; dilution 1:200; eBioscience™), and anti-Connexin-43 (mouse monoclonal antibody CX-1B1; dilution 1:200; eBioscience™). All of the antibodies were diluted in PBS + 0.15% Tween (PBSt). Protein detection was performed with the Immun-Star WesternC kit (BioRad Lab, Hercules, CA, USA), and images were acquired; quantitative densitometry was performed using the ChemiDoc XRS + System (Bio-Rad). The data are expressed as relative optical density (R.O.D.) and normalized against α -tubulin expression (mouse anti- α -tubulin, 1:1000, Merckmillipore, Burlington, MA, USA). α -tubulin was chosen as the reference because, even if its polymerization is altered by microgravity, its amount into the cell results in a stable signal through microgravity experiments in the time lapse considered in the present research [18].

4.7. Statistical Analysis

For the morphometric analysis, statistical analysis was performed using ANOVA followed by a post hoc Bonferroni test. The normality of the data distribution was assured by the Kolgomorov–Smirnov test. p values < 0.05 were considered significant. The data are reported as mean \pm SD.

5. Conclusions

In conclusion, microgravity exerts an inhibitory effect on principal cytoskeletal dynamic components such as GFAP, vinculin, and Cx43, which are all related to proliferative and metastatic behaviors of glioma cells. Although in the present research, direct experiments *in vitro* or *in vivo* on the migration and metastatic behavior of C6 cells were not planned, our findings strongly address the indication of microgravity as a potential anti-tumoral countermeasure.

Author Contributions: Conceptualization, M.S. and M.A.M.; methodology, V.B. and C.L.; validation, M.S., V.M. and F.D.; formal analysis, M.S., V.B. and C.L.; investigation, V.M., M.S., V.B. and C.L.; resources, M.S., M.A.M. and F.D.; data curation, M.S., V.B. and C.L.; writing—original draft preparation, M.S. and V.M.; writing—review and editing, M.A.M. and F.D.; visualization, M.S. and V.M.; supervision, M.A.M. and F.D.; project administration, M.S. and M.A.M.; funding acquisition, M.S. and M.A.M. All authors have read and agreed to the published version of the manuscript.

Funding: This research was performed thanks to academic funds—“UPO FAR2017_Sabbatini” and “UPO FAR2017_Masini” and “THOR—Associazione per il Sostegno alla Ricerca ONLUS”.

Data Availability Statement: Our study is a morphological and observational study based on the distribution of specific proteins; therefore, the minimal data set is the image collection shown in the article. Further raw data will be available upon reasonable request to the authors.

Acknowledgments: The authors thank the ASI (Italian Space Agency) for suggestions and critical support.

Conflicts of Interest: The authors declare no conflict of interest. The funders had no role in the design of the study; in the collection, analyses, or interpretation of data; in the writing of the manuscript; or in the decision to publish the results.

References

1. Laranjeiro, R.; Harinath, G.; Pollard, A.K.; Gaffney, C.J.; Deane, C.S.; Vanapalli, S.A.; Etheridge, T.; Szewczyk, N.J.; Driscoli, M. Spaceflight affects neuronal morphology and alters transcellular degradation of neuronal debris in adult *Caenorhabditis elegans*. *iScience* **2021**, *24*, 102105. [[CrossRef](#)] [[PubMed](#)]
2. Lei, X.; Cao, Y.; Zhang, Y.; Qian, Z.; Liu, F.; Zhang, T.; Zhou, J.; Gu, Y.; Xia, G.; Duan, E. Effect of microgravity on proliferation and differentiation of embryonic stem cells in an automated culturing system during the TZ-1 space mission. *Cell Prolif.* **2018**, *51*, e12466. [[CrossRef](#)] [[PubMed](#)]
3. Prasad, B.; Grimm, D.; Strauch, S.M.; Erzinger, G.S.; Corydon, T.J.; Lebert, M.; Magnusson, N.E.; Infanger, M.; Richter, P.; Krüger, M. Influence of Microgravity on Apoptosis in Cells, Tissues, and Other Systems In Vivo and In Vitro. *Int. J. Mol. Sci.* **2020**, *21*, 9373. [[CrossRef](#)] [[PubMed](#)]
4. Lin, X.; Zhang, K.; Wei, D.; Tian, Y.; Gao, Y.; Chen, Z.; Qian, A. The Impact of Spaceflight and Simulated Microgravity on Cell Adhesion. *Int. J. Mol. Sci.* **2020**, *21*, 3031. [[CrossRef](#)]
5. Uva, B.M.; Masini, M.A.; Sturla, M.; Prato, P.; Passalacqua, M.; Giuliani, M.; Tagliaferro, G.; Strollo, F. Clinorotation-induced weightlessness influences the cytoskeleton of glial cells in culture. *Brain Res.* **2002**, *934*, 132–139. [[CrossRef](#)] [[PubMed](#)]
6. Leguy, C.A.D.; Delfos, R.; Pourquie, M.J.B.M.; Poelma, C.; Westerweel, J.; van Loon, J.J.W.A. Fluid dynamics during Random Positioning Machine micro-gravity experiments. *Adv. Space Res.* **2017**, *59*, 3045–3057. [[CrossRef](#)]
7. Wuest, S.L.; Richard, S.; Kopp, S.; Grimm, D.; Egli, M. Simulated Microgravity: Critical Review on the Use of Random Positioning Machines for Mammalian Cell Culture. *BioMed Res. Int.* **2015**, *2015*, 971474. [[CrossRef](#)]
8. Nassef, M.Z.; Melnik, D.; Kopp, S.; Sahana, J.; Infanger, M.; Lützenberg, R.; Relja, B.; Wehland, M.; Grimm, D.; Krüger, M. Breast Cancer Cells in Microgravity: New Aspects for Cancer Research. *Int. J. Mol. Sci.* **2020**, *21*, 7345. [[CrossRef](#)]
9. Cortés-Sánchez, J.L.; Callant, J.; Krüger, M.; Sahana, J.; Kraus, A.; Baselet, B.; Infanger, M.; Baatout, S.; Grimm, D. Cancer Studies under Space Conditions: Finding Answers Abroad. *Biomedicine* **2021**, *10*, 25. [[CrossRef](#)]
10. Chung, J.H.; Ahn, C.B.; Son, K.H.; Yi, E.; Son, H.S.; Kim, H.S.; Lee, S.H. Simulated microgravity effects on non small cell lung cancer cell proliferation and migration. *Aerosp. Med. Hum. Perform.* **2017**, *88*, 82–89. [[CrossRef](#)]
11. Jessup, J.M.; Goodwin, T.J.; Garcia, R.; Pellis, N. STS-70: First flight of EDU-1. *Vitr. Cell. Dev. Biol.* **1996**, *32*, 13A.
12. Chen, J. Tumor cells in microgravity. In *Into Space—A Journey of How Humans Adapt and Live in Microgravity*; Russomano, T., Rehnberg, L., Eds.; IntechOpen: Rijeka, Croatia, 2018.
13. Sahebi, R.; Aghaei, M.; Halvaei, S.; Alizadeh, A. The role of microgravity in cancer: A dual-edge sword. *Multidiscip. Cancer Investig.* **2017**, *1*, 1–5. [[CrossRef](#)]
14. Ahn, C.B.; Lee, J.H.; Han, D.G.; Kang, H.-W.; Lee, S.-H.; Lee, J.-I.; Son, K.H.; Lee, J.W. Simulated microgravity with floating environment promotes migration of non-small cell lung cancers. *Sci. Rep.* **2019**, *9*, 14553. [[CrossRef](#)]
15. Chang, D.; Xu, H.; Guo, Y.; Jiang, X.; Liu, Y.; Li, K.; Pan, C.; Yuan, M.; Wang, J.; Li, T.; et al. Simulated microgravity alters the metastatic potential of a human lung adenocarcinoma cell line. *Vitr. Cell. Dev. Biol. Anim.* **2013**, *49*, 170–177. [[CrossRef](#)] [[PubMed](#)]
16. Krüger, M.; Melnik, D.; Kopp, S.; Buken, C.; Sahana, J.; Bauer, J.; Wehland, M.; Hemmersbach, R.; Corydon, T.J.; Infanger, M.; et al. Fighting Thyroid Cancer with Microgravity Research. *Int. J. Mol. Sci.* **2019**, *20*, 2553. [[CrossRef](#)] [[PubMed](#)]
17. Fife, C.M.; McCarroll, J.A.; Kavallaris, M. Movers and shakers: Cell cytoskeleton in cancer metastasis. *Br. J. Pharmacol.* **2014**, *171*, 5507–5523, Erratum in *Br. J. Pharmacol.* **2017**, *174*, 116. [[CrossRef](#)]
18. Masini, M.A.; Strollo, F.; Ricci, F.; Pastorino, M.; Uva, B.M. Microtubules disruption and repair phenomena in cultured glial cells under microgravity. *Grav. Space Biol.* **2006**, *19*, 149–150.
19. Ulbrich, C.; Pietsch, J.; Grosse, J.; Wehland, M.; Schulz, H.; Saar, K.; Hübner, N.; Hauslage, J.; Hemmersbach, R.; Braun, M.; et al. Differential gene regulation under altered gravity conditions in follicular thyroid cancer cells: Relationship between the extracellular matrix and the cytoskeleton. *Cell. Physiol. Biochem.* **2011**, *28*, 185–198. [[CrossRef](#)]
20. Tan, X.; Xu, A.; Zhao, T.; Zhao, Q.; Zhang, J.; Fan, C.; Deng, Y.; Freywald, A.; Genth, H.; Xiang, J. Simulated microgravity inhibits cell focal adhesions leading to reduced melanoma cell proliferation and metastasis via FAK/RhoA-regulated mTORC1 and AMPK pathways. *Sci. Rep.* **2018**, *28*, 3769. [[CrossRef](#)]
21. Kis, D.; Szivos, L.; Rekecki, M.; Shukir, B.S.; Mate, A.; Hideghety, K.; Barzo, P. Predicting the true extent of glioblastoma based on probabilistic tractography. *Front. Neurosci.* **2022**, *16*, 886465. [[CrossRef](#)]
22. Yan, H.; Parsons, D.W.; Jin, G.; McLendon, R.; Rasheed, B.A.; Yuan, W.; Kos, I.; Batinic-Haberle, I.; Jones, S.; Riggins, G.J.; et al. IDH1 and IDH2 mutations in gliomas. *N. Engl. J. Med.* **2009**, *360*, 765–773. [[CrossRef](#)] [[PubMed](#)]
23. Wirsching, H.G.; Galanis, E.; Weller, M. Glioblastoma. *Handb. Clin. Neurol.* **2016**, *134*, 381–397. [[PubMed](#)]
24. Deng, B.; Liu, R.; Tian, X.; Hans, Z.; Chen, J. Simulated microgravity inhibits the viability and migration of glioma via FAK/RhoA/Rock and FAK/Nek2 signaling. *Vitr. Cell. Dev. Biol. Anim.* **2019**, *55*, 260–271. [[CrossRef](#)]

25. Giakoumettis, D.; Kritis, A.; Foroglou, N. C6 cell line: The gold standard in glioma research. *Hippokratia* **2018**, *22*, 105–112. [[PubMed](#)]
26. Rutka, J.T.; Murakami, M.; Dirks, P.B.; Hubbard, S.L.; Becker, L.E.; Fukuyama, K.; Jung, S.; Tsugu, A.; Matsuzawa, K. Role of glial filaments in cells and tumors of glial origin: A review. *J. Neurosurg.* **1997**, *87*, 420–430. [[CrossRef](#)]
27. Borgon, R.A.; Vonrhein, C.; Bricogne, G.; Bois, P.R.; Izard, T. Crystal structure of human vinculin. *Structure* **2004**, *12*, 1189–1197. [[CrossRef](#)]
28. Cottin, S.; Ghani, K.; Caruso, M. Bystander effect in glioblastoma cells with a predominant cytoplasmic localization of connexin43. *Cancer Gene Ther.* **2008**, *15*, 823–831. [[CrossRef](#)]
29. Uceda-Castro, R.; van Asperen, J.V.; Vennin, C.; Sluijs, J.A.; van Bodegraven, E.J.; Margarido, A.S.; Robe, P.A.J.; van Rheen, J.; Hol, E.M. GFAP splice variants fine-tune glioma cell invasion and tumour dynamics by modulating migration persistence. *Sci. Rep.* **2022**, *12*, 424. [[CrossRef](#)]
30. Huang, D.L.; Bax, N.A.; Buckley, C.D.; Weis, W.I.; Dunn, A.R. Vinculin forms a directionally asymmetric catch bond with F-actin. *Science* **2017**, *357*, 703. [[CrossRef](#)]
31. Bays, J.L.; Peng, X.; Tolbert, C.E.; Guilluy, C.; Angell, A.E.; Pan, Y.; Superfine, R.; Burrige, K.; DeMali, K.A. Vinculin phosphorylation differentially regulates mechanotransduction at cell-cell and cell-matrix adhesions. *J. Cell Biol.* **2014**, *205*, 251. [[CrossRef](#)]
32. Seddiki, R.; Narayana, G.H.N.S.; Strale, P.O.; Balcioglu, H.E.; Peyret, G.; Yao, M.; Le, A.P.; Teck Lim, C.; Yan, J.; Ladoux, B.; et al. Force-dependent binding of vinculin to α -catenin regulates cell-cell contact stability and collective cell behavior. *Mol. Biol. Cell* **2018**, *29*, 380. [[CrossRef](#)]
33. Rosowski, K.A.; Boltianskiy, R.; Xiang, Y.; Van den Dries, K.; Schwartz, M.A.; Dufresne, E.R. Vinculin and the mechanical response of adherent fibroblasts to matrix deformation. *Sci. Rep.* **2018**, *8*, 17967. [[CrossRef](#)]
34. Rothenberg, K.E.; Scott, D.W.; Christoforou, N.; Hoffman, B.D. Vinculin Force-Sensitive Dynamics at Focal Adhesions Enable Effective Directed Cell Migration. *Biophys. J.* **2018**, *114*, 1680. [[CrossRef](#)] [[PubMed](#)]
35. Wang, F.; Fang, M.; Kong, M.; Wang, C.; Xu, Y. Vinculin presents unfavorable prediction in ovarian cancer and prevents proliferation and migration of ovarian cancer cells. *J. Biochem. Mol. Toxicol.* **2020**, *5*, e22525. [[CrossRef](#)] [[PubMed](#)]
36. Li, T.; Guo, H.; Song, Y.; Zhao, X.; Shi, Y.; Lu, Y.; Hu, S.; Nie, Y.; Fan, D.; Wu, K. Loss of vinculin and membrane-bound β -catenin promotes metastasis and predicts poor prognosis in colorectal cancer. *Mol. Cancer* **2014**, *13*, 263. [[CrossRef](#)] [[PubMed](#)]
37. Toma-Jonik, A.; Widlak, W.; Korfanty, J.; Cichon, T.; Smolarczyk, R.; Gogler-Piglowska, A.; Widlak, P.; Vydra, N. Active heat shock transcription factor 1 supports migration of the melanoma cells via vinculin down-regulation. *Cell. Signal.* **2015**, *27*, 394. [[CrossRef](#)] [[PubMed](#)]
38. Mierke, C.T. The role of vinculin in the regulation of the mechanical properties of cells. *Cell. Biochem. Biophys.* **2009**, *53*, 115–126. [[CrossRef](#)] [[PubMed](#)]
39. Rubashkin, M.G.; Cassereau, L.; Bainer, R.; DuFort, C.C.; Yui, Y.; Ou, G.; Paszek, M.J.; Davidson, M.W.; Chen, Y.Y.; Weaver, V.M. Force engages vinculin and promotes tumor progression by enhancing PI3K activation of phosphatidylinositol (3,4,5)-triphosphate. *Cancer Res.* **2014**, *74*, 4597–4611. [[CrossRef](#)] [[PubMed](#)]
40. Zheng, X.; Xu, H.; Gong, L.; Cao, D.; Jin, T.; Wang, Y.; Pi, J.; Yang, Y.; Yi, X.; Liao, D.; et al. Vinculin orchestrates prostate cancer progression by regulating tumor cell invasion, migration, and proliferation. *Prostate* **2021**, *81*, 347–356. [[CrossRef](#)]
41. Chantaravisoot, N.; Wongkongkathep, P.; Loo, J.A.; Michel, P.S.; Tamanoi, F. Significance of filamin A in mTORC2 function in glioblastoma. *Mol. Cancer* **2014**, *14*, 127. [[CrossRef](#)]
42. Yang, S.; Zhang, J.J.; Huang, X. Orai1 and STIM1 Are Critical for Breast Tumor Cell Migration and Metastasi Cancer. *Cell* **2009**, *15*, 124.
43. Shi, Z.; Rao, W.; Wang, H.; Wang, N.; Si, J.; Zhao, J.; Li, J.; Wang, Z. Modeled microgravity suppressed invasion and migration of human glioblastoma U87 cells through downregulating store-operated calcium entry. *Biochem. Biophys. Res. Commun.* **2015**, *457*, 378. [[CrossRef](#)] [[PubMed](#)]
44. Zhu, M.; Lv, B.; Ge, W.; Cui, Z.; Zhao, K.; Feng, Y.; Yang, X. Suppression of store-operated Ca^{2+} entry regulated by silencing Orai1 inhibits C6 glioma cell motility via decreasing Pyk2 activity and promoting focal adhesion. *Cell Cycle* **2020**, *19*, 3468. [[CrossRef](#)] [[PubMed](#)]
45. Dong, H.; Zhou, X.-W.; Wang, X.; Yang, Y.; Luo, J.-W.; Liu, Y.-H.; Mao, Q. Complex role of connexin 43 in astrocytic tumors and possible promotion of glioma-associated epileptic discharge (Review). *Mol. Med. Rep.* **2017**, *16*, 7890–7900. [[CrossRef](#)] [[PubMed](#)]
46. Sharrow, A.C.; Li, Y.; Micsenyi, A.; Griswold, R.D.; Wells, A.; Monga, S.S.; Blair, H.C. Modulation of osteoblast gap junction connectivity by serum, TNF α , and TRAIL. *Exp. Cell. Res.* **2008**, *314*, 297–308. [[CrossRef](#)] [[PubMed](#)]
47. Taberero, A.; Gangoso, E.; Jaraíz-Rodríguez, M.; Medina, J.M. The role of connexin43-*Src* interaction in astrocytomas: A molecular puzzle. *Neuroscience* **2016**, *323*, 183–194. [[CrossRef](#)] [[PubMed](#)]
48. Zhang, W.; Nwagwu, C.; Le, D.M.; Yong, V.W.; Song, H.; Couldwell, W.T. Increased invasive capacity of connexin43-overexpressing malignant glioma cells. *J. Neurosurg.* **2003**, *99*, 1039–1046. [[CrossRef](#)]
49. McDonough, W.S.; Johansson, A.; Joffe, H.; Giese, A.; Berens, M.E. Gap junction intercellular communication in gliomas is inversely related to cell motility. *Int. J. Dev. Neurosci.* **1999**, *17*, 601–611. [[CrossRef](#)]
50. Soroceanu, L.; Manning, T.; Sontheimer, H. Reduced expression of connexin-43 and functional gap junction coupling in human gliomas. *Glia* **2001**, *33*, 107–117. [[CrossRef](#)]

51. Pu, P.; Xia, Z.; Yu, S.; Huang, Q. Altered expression of Cx43 in astrocytic tumors. *Clin. Neurol. Neurosurg.* **2004**, *107*, 49–54. [[CrossRef](#)]
52. Osswald, M.; Jung, E.; Sahm, F.; Solecki, G.; Venkataramani, V.; Blaes, J.; Weil, S.; Horstmann, H.; Wiestler, B.; Syed, M.; et al. Brain tumour cells interconnect to a functional and resistant network. *Nature* **2015**, *528*, 93–98. [[CrossRef](#)] [[PubMed](#)]
53. Sin, W.C.; Crespin, S.; Mesnil, M. Opposing roles of connexin43 in glioma progression. *Biochim. Biophys. Acta* **2012**, *1818*, 2058–2067. [[CrossRef](#)] [[PubMed](#)]
54. Hong, X.; Sin, W.C.; Harris, A.L.; Naus, C.C. Gap junctions modulate glioma invasion by direct transfer of microRNA. *Oncotarget* **2015**, *6*, 15566–15577. [[CrossRef](#)]
55. Sin, W.C.; Aftab, Q.; Bechberger, J.F.; Leung, J.H.; Chen, H.; Naus, C.C. Astrocytes promote glioma invasion via the gap junction protein connexin43. *Oncogene* **2016**, *35*, 1504–1516. [[CrossRef](#)] [[PubMed](#)]
56. Crespin, S.; Fromont, G.; Wager, M.; Levillain, P.; Cronier, L.; Monvoisin, A.; Defamie, N.; Mesnil, M. Expression of a gap junction protein, connexin43, in a large panel of human gliomas: New insights. *Cancer Med.* **2016**, *5*, 1742–1752. [[CrossRef](#)]
57. Yang, Y.M.; Seki, E. Global Spread of a Local Fire: Transmission of Endoplasmic Reticulum Stress via Connexin 43. *Cell. Metab.* **2021**, *33*, 229–230. [[CrossRef](#)]
58. McCutcheon, S.; Spray, D.C. Glioblastoma-Astrocyte Connexin 43 Gap Junctions Promote Tumor Invasion. *Mol. Cancer Res.* **2022**, *20*, 319–331. [[CrossRef](#)]
59. Kotini, M.; Barriga, E.H.; Leslie, J.; Gentzel, M.; Rauschenberger, V.; Schambony, A.; Mayor, R. Gap junction protein Connexin-43 is a direct transcriptional regulator of N-cadherin in vivo. *Nat. Commun.* **2018**, *9*, 3846, Erratum in *Nat. Commun.* **2018**, *9*, 4633. [[CrossRef](#)]
60. Ruggieri, I.N.C.; Cicero, A.M.; Issa, J.P.M.; Feldman, S. Bone fracture healing: Perspectives according to molecular basis. *J. Bone Mineral Metab.* **2021**, *39*, 311–331. [[CrossRef](#)]
61. Brungs, S.; Egli, M.; Wuest, S.L.M.; Christianen, P.C.; van Loon, J.J.W.A.; Ngo, A.; Thu, J.; Hemmersbach, R. Facilities for Simulation of Microgravity in the ESA Ground-Based Facility Programme. *Micrograv. Sci. Technol.* **2016**, *28*, 191–203. [[CrossRef](#)]
62. Wuest, S.L.; Stern, P.; Casartelli, E.; Egli, M. Fluid Dynamics Appearing during Simulated Microgravity Using Random Positioning Machines. *PLoS ONE* **2017**, *12*, e0170826. [[CrossRef](#)] [[PubMed](#)]

Disclaimer/Publisher’s Note: The statements, opinions and data contained in all publications are solely those of the individual author(s) and contributor(s) and not of MDPI and/or the editor(s). MDPI and/or the editor(s) disclaim responsibility for any injury to people or property resulting from any ideas, methods, instructions or products referred to in the content.